



Published in final edited form as:

Eur J Med Chem. 2015 October 20; 103: 123–132. doi:10.1016/j.ejmech.2015.08.041.

Synthesis and biological evaluation of novel 4,5-disubstituted 2*H*-1,2,3-triazoles as *cis*-constrained analogues of combretastatin A-4

Nikhil R. Madadi^a, Narsimha R. Penthala^a, Kevin Howk^{a,b}, Amit Ketkar^c, Robert L. Eoff^c, Michael J. Borrelli^b, and Peter A. Crooks^{a,*}

^aDepartment of Pharmaceutical Sciences, College of Pharmacy, University of Arkansas for Medical Sciences, Little Rock, AR 72205-7199, USA

^bDepartment of Radiology, College of Medicine, University of Arkansas for Medical Sciences, Little Rock, AR 72205-7199, USA

^cDepartment of Biochemistry and Molecular Biology, University of Arkansas for Medical Sciences, Little Rock, AR 72205-7199, U.S.A.

Abstract

A series of combretastatin A-4 (CA-4) analogues have been prepared from (*Z*)-substituted diarylacrylonitriles (**1a–1p**) obtained in a two-step synthesis from appropriate arylaldehydes and acrylonitriles. The resulting 4,5-disubstituted 2*H*-1,2,3-triazoles were evaluated for their anti-cancer activities against a panel of 60 human cancer cell lines. The diarylacrylonitrile analogue **2l** exhibited the most potent anti-cancer activity in the screening studies, with GI₅₀ values of <10 nM against almost all the cell lines in the human cancer cell panel and TGI values of <10nM against cancer cell lines SF-539, MDA-MB-435, OVCAR-3 and A498. Furthermore, *in silico* docking studies of compounds **2l**, **2e** and **2h** within the active site of tubulin were carried out in order to rationalize the mechanism of anti-cancer properties of these compounds. From the *in silico* studies, compound **2e** was predicted to have better affinity for the colchicine binding site on tubulin compared to compounds **2l** and **2h**. Analogue **2e** was also evaluated for its anti-cancer activity by colony formation assay against 9LSF rat gliosarcoma cells and afforded an LD₅₀ of 7.5 nM. A cell cycle redistribution assay using analogue **2e** was conducted to further understand the mechanism of action of these CA-4 analogues. From this study, analogues **2e** and **2l** were the most potent anti-cancer agents in this structural class, and were considered lead compounds for further development as anti-cancer drugs.

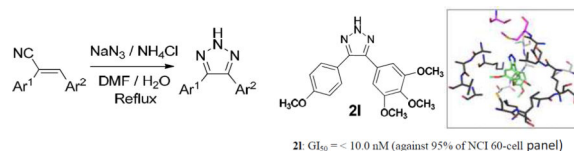
Graphical Abstract

*Corresponding author. Tel.: +1-501-686-6495; fax: +1-501-686-6057; pacrooks@uams.edu (P. A. Crooks).

Publisher's Disclaimer: This is a PDF file of an unedited manuscript that has been accepted for publication. As a service to our customers we are providing this early version of the manuscript. The manuscript will undergo copyediting, typesetting, and review of the resulting proof before it is published in its final citable form. Please note that during the production process errors may be discovered which could affect the content, and all legal disclaimers that apply to the journal pertain.

Appendix A. Supplementary data

Supplementary data related to this article can be found at <http://dx.doi.org/10.1016/...>



Keywords

Novel 4,5-disubstituted 2H-1,2,3-triazoles; Anti-cancer activity; Gliosarcoma cells; *In silico* docking studies; Cell cycle redistribution assay

1. Introduction

Cancer is the second most life threatening disease after cardiovascular disease, affecting more than six million people per year worldwide. Although, significant research has done to date to treat cancer, there is still a lack of effective chemotherapeutic treatment to cure it completely with minimal side effects. Also, considerable effort has been put into identifying molecules with anti-cancer properties from both natural and synthetic sources. More than 60% of the anti-cancer drugs currently available are from natural sources [1]. The search for potent semi synthetically derived anti-cancer agents from the parent natural products continues to be an important part of drug discovery process. Anti-mitotic agents are a major class of cytotoxic drugs for the treatment of cancer and drugs that target microtubule/tubulin dynamics are widely used in cancer chemotherapy [2].

There are three major binding sites for tubulin; i.e. the vinca, taxane and colchicine domains. Vinca alkaloids, such as vincristine and vinblastine, bind to the vinca domain inhibiting the assembly of microtubule structures and arresting mitosis [3]. Paclitaxel acts at the taxane domain stabilizing microtubules and interfering with the normal breakdown of microtubules during mitosis [4]. Our area of interest focused on the colchicine binding site. Colchicine binds to tubulin and inhibits microtubule polymerization. Anti-mitotic agents such as combretastatin A-4 (CA-4) bind at the colchicine domain of tubulin, and have received much attention in recent years; CA-4P, the water soluble phosphate salt of CA-4 is currently in phase III clinical trial for anaplastic thyroid cancer, and is also in phase II trials for polypoidal choroidal vasculopathy and neovascular age-related macular degeneration [5, 6].

CA-4 is classified as a *cis*-stilbene originating from the South African willow tree *combretum caffrum*. CA-4 functions as a microtubule targeting agent interfering with microtubule dynamics and perturbs the mitotic cycle [7]. When compared to colchicine, the vascular disrupting effects of CA-4 are well below the maximum tolerable dose with fewer side effects *in vivo* [8]. However, CA-4 suffers from stability issues because of its tendency to undergo *cis-trans* double bond isomerism in solution. CA-4 is a *cis*-configured stilbene which is readily converted to the thermodynamically more stable, but less potent *trans*-isomer [9]. Extensive studies have been conducted in attempts to stabilize the *cis* configuration by replacing the olefinic double bond with heterocyclic ring systems such as β -lactam, azetidone, thiazole, tetrazole, imidazole, pyrazole, oxazolone, triazole, furanone moieties [10–15].

In the work described herein, we report on the synthesis of series of novel *cis*-constrained 4,5-disubstituted 2*H*-1,2,3-triazole analogues of CA-4. The 2*H*-1,2,3-triazole ring system was designed to not only halt *cis-trans* isomerization, but also improve the drug likeness of the resulting CA-4 analogue, along with providing scope for further structural diversification. Evaluation of these novel triazole analogues of CA-4 against a panel of 60 human tumor cell lines has been performed, along with cell cycle redistribution assays. The molecular mechanism responsible for the of the anti-cancer activity of the three most potent molecules, **2e**, **2h** and **2l**, has been investigated by performing molecular docking studies with the target molecule, tubulin.

2. Results and discussion

2.1. Drug synthesis

The general procedure for the synthesis of the 4,5-disubstituted 2*H*-1,2,3-triazole CA-4 analogues is illustrated in Scheme 1. In the first step, a series of (*Z*)-substituted diarylacrylonitrile analogues were synthesized by reacting substituted benzyl carbaldehydes with their corresponding substituted phenylacetonitriles in 5% NaOMe in methanol. The reaction mixture was stirred at room temperature for 2–3 hours, during which time the desired product precipitated out of the solution. The resulting product was then filtered, washed with water, and dried to yield the final compound; yields ranged from 70–95 % (Scheme 1) [16].

In the second step, 4,5-disubstituted-2*H*-1,2,3-triazoles were obtained by refluxing a mixture of the (*Z*)-2,3-diarylacrylonitrile (**1a–1s**) from step 1 with NaN₃, and NH₄Cl in a mole ratio of 1:3:3 in 10:1 volumes of DMF/H₂O for 5–12 h. The reaction mixture was monitored by TLC, and when the starting material had completely disappeared, cold water was added and the mixture stirred over 10–15 min, during which the final product precipitated out and was filtered off, washed with water and dried. In cases where there was an absence of a precipitate, the product was extracted into ethyl acetate, the organic extract washed with copious amounts of water, and the resulting organic liquor evaporated to dryness on a rotary evaporator. The residue obtained was purified by flash column chromatography to afford the corresponding triazole (Scheme 1) [17]. The structure and purity of the triazole derivatives were verified by ¹H, ¹³C-NMR spectroscopy, high resolution mass spectroscopy and X-ray crystallography [17–20].

Based on previous SAR studies on *cis* constrained CA-4 analogues, triazole analogues initially chosen for synthesis contained the 3,4,5-trimethoxyphenyl moiety (Ring A) and a variably substituted aryl or heteroaryl moiety (Ring B) [7, 21]. In later structural modifications we introduced halogeno, nitro and hydroxyl functionalities ring A.

2.2. Biological Evaluation

2.2.1. Anti-cancer activity against a panel of NCI 60 human cancer cells—The sulforhodamine B (SRB) assay procedure described by Rubinstein et al. was used to screen the CA-4 analogues **2a–2s** against a panel of 60 human tumor cell lines [22]. Growth inhibitory or cytotoxic effects were measured by percentage growth (PG), which is

proportional to optical density (OD) [23, 24]. OD measurements of SRB-derived color prior to and 48 hrs after exposure of cells to the test compound or vehicle control were recorded. Ten compounds (**2c–2e**, **2g**, **2j**, **2l–2n**, **2r**, and **2s**) were initially identified as “hits” after screening at all the analogues at 10^{-5} M concentration. These single concentration results are presented in the supplementary data section. The screening protocol utilized to identify a hit was 60% growth inhibition at 10^{-5} M in at least eight cell lines from the panel of 60 cell lines. Compounds that met these criteria were then selected for a complete dose response study at five different concentrations, viz. 10^{-4} M, 10^{-5} M, 10^{-6} M, 10^{-7} M and 10^{-8} M. Six of the preliminary hits (**2d**, **2g**, **2h**, and **2l–2n**) were evaluated in the full dose-response studies had effective GI_{50} and TGI (Total growth inhibition) values against a variety of human tumor cell lines (Table 2). All the compounds have LD_{50} values >100 μ M against most of the human cancer cell lines, indicating that the compounds are anti-proliferative.

Analogue **2l** had impressive GI_{50} values of less than 10 nM against almost all of the 60 cancer cell lines in the panel, except for melanoma cancer cell line UACC-62, and colon cancer cell lines COLO 205 and HCC-2998. Compound **2l** also showed potent anti-proliferative activity with TGI values of <10 nM against CNS cancer cell line SF-539, melanoma cell MDA-MB-435, ovarian cancer cell line OVCAR-3, and renal cancer cell line A498.

Analogue **2m** exhibited potent growth inhibitory activity with $GI_{50} <10$ nM against leukemia cancer cell lines K-562 and SR, non-small cell lung cancer cell line HOP-92, colon cancer cell lines HCT-116 and HCT-15, melanoma cancer lines M14 and UACC-62, ovarian cancer cell line NCI/ADR-RES, and renal cancer cell line A498. Melanoma cancer cell line MDA-MB-435 appeared to be the most sensitive to the growth inhibitory effects of **2m**, exhibiting a TGI value of 10 nM.

Analogue **2h** also showed potential growth inhibitory properties with $GI_{50} <10$ nM against leukemia cancer cell lines K-562 and SR, non-small cell lung cancer cell line HOP-92, colon cancer cell lines HCT-116, HCT-15, KM-12, and SW-620, CNS cancer cell lines SF-295, SF-539, and SNB-75, melanoma cancer lines M14, MDA-MB-435, and SK-MEL-2, ovarian cancer cell lines NCI/ADR-RES, and SK-OV-3, renal cancer cell lines A498, ACHN, CAKI-1, and UO-31, and breast cancer cell line MCF-7.

From the above screening studies, analogue **2l** was considered to be a lead candidate, since it exhibited very promising GI_{50} and TGI values against a wide variety of both hematological and solid tumor cell types. However, *in silico* tubulin docking studies carried out with the triazole analogues revealed slightly better tubulin binding affinity for compound **2e** compared to **2l**. Unfortunately, analogue **2e**, which is the triazole-derived form of the CA4 molecule, was not selected for the 60 human cancer cell screen. We therefore evaluated **2e** for its anti-cancer activity by colony formation assay against 9LSF rat gliosarcoma cells.

2.2.2 Colony formation assay results for **2e** utilizing 9LSF rat gliosarcoma

cells—9LSF cells were acquired from the laboratory of Dennis Deen, Ph.D. (Brain Tumor Research Center, University of California, San Francisco). Cells were exposed to **2e** at concentrations of 1 nM, 3 nM, 10 nM, 30 nM, 100 nM, 1 μ M, or 10 μ M for 24 hours prior to

seeding for the colony formation assay. Cells were then trypsinized, counted, seeded into 25 cm² flasks, and incubated at 37°C to form colonies [25]. All conditions were seeded in triplicate. Flasks that were plated with less than 50,000 cells were previously plated with 50,000 lethally irradiated A549 cells to serve as feeders [26]. Flasks were removed from incubation when colonies were large enough to count (>50 cells). Colonies were then fixed and stained with crystal violet, rinsed, allowed to dry, and counted. The protocol was run in triplicate, and results averaged, with error representing SEM. The LD₅₀ value for **2e** was determined to be 7.5 nM using SigmaPlot 11.

2.2.3 Cell cycle redistribution using 2e—9LSF cells were exposed to 50 nM **2e** or 50 nM colchicine (COL) for 24 hrs *in vitro*, along with controls. Cells were then trypsinized, counted, rinsed with PBS, and fixed using ice-cold 70% EtOH in PBS at 10⁶ cells/mL. Samples were stored at 4°C prior to flow cytometry analysis; 10⁶ cells from each condition were then pelleted and rinsed thrice with PBS. Samples were resuspended in 1 mL PBS, to which 1 µL propidium iodide (PI, 12.5 mg/mL in DMSO) was added. Samples were exposed to PI for 2 minutes at room temperature, then immediately analyzed by flow cytometry (Cell Lab Quanta SC, Beckman Coulter, Inc., Brea, CA.) The protocol was run in triplicate. Cell cycle distributions were analyzed using FCS Express 3 (De Novo Software, Glendale, CA).

3. *In silico* molecular docking studies

Two analogues (**2h** and **2l**) from the 60 human cancer cell panel screens, and analogue **2e**, (GI₅₀ <10 nM) were chosen for molecular docking studies utilizing the available crystal structure of tubulin, in order to understand the possible mechanism of their action as inhibitors of tubulin polymerization. Atomic coordinates for tubulin (PDB 1SA0) were downloaded from the protein structure database (www.rcsb.org/pdb). Colchicine was removed from the coordinate file and the coordinates of only chains A and B, corresponding to a α,β -tubulin heterodimer were used for the docking studies. Atomic coordinates for all compounds were generated using MarvinSketch (ChemAxon), and both the ligand and target protein coordinate files were prepared for docking using the Dock Prep module in the UCSF-Chimera package (<http://www.cgl.ucsf.edu/chimera>). Docking was performed using SwissDock (<http://www.swissdock.ch/>), based on the docking algorithm EADock DSS [27]. Docking was performed using protocols established in our previous studies [16]. Use of the most exhaustive and unbiased option in SwissDock ensured the sampling of the maximum number of binding modes for each molecule. The best hits based on the SwissDock FullFitness scoring function (FF) from three repeated docking runs were considered further.

All three compounds docked almost exclusively to the colchicine-binding pocket on the α,β -tubulin heterodimer. This indicates that the mode of inhibition of tubulin polymerization by these three molecules is similar to that of colchicine and CA-4, and that the introduction of a triazole ring in place of the *cis*-olefinic bond still retains potent tubulin binding properties. Among the three molecules examined, **2e** had the most number of ‘outlier’ poses that docked in non-colchicine binding, surfaceexposed pockets. However, 86% of the docked poses were still localized at the colchicine-pocket. In the case of **2h** and **2l**, this number was 95% and 99%, respectively (Fig. 4).

All three molecules were primarily stabilized through several van der Waals' contacts with residues from the α - and β -subunits of tubulin. Compound **2e** was found to interact with 13 β residues and 5 α residues of tubulin (Fig 5). In contrast, both molecules **2h** and **2l**, besides sharing all the contact residues of **2e**, made additional contacts with Met259 and Thr314 of the β - subunit of tubulin (Fig 5B). This is reflected in the FF and ΔG scores of the three compounds (Table 3), with the FF score and free energy values for **2l** and **2h** being higher than that for **2e**. Both scores followed the order: **2e** < **2h** < **2l**.

4. Conclusions

A series of 4,5-disubstituted 2H-1,2,3-triazoles designed as CA4 analogues were synthesized from corresponding (Z)-substituted diarylacrylonitriles (**1a–1s**). The synthesis represents a facile and efficient reaction procedure for the preparation of 4,5-diaryl-2H-1,2,3-triazoles in modest to good yields. The resulting 4,5-disubstituted 2H-1,2,3-triazoles were evaluated for their anticancer properties against a panel of 60 human cancer cell lines. The diarylacrylonitrile analogue **2l** exhibited the most potent anticancer activity in the cancer cell screening studies, with GI₅₀ values of <10 nM against almost all the cell lines in the panel. Analogue **2l** also exhibited promising TGI values of <10 nM against CNS cancer cell line SF-539, melanoma cell MDA-MB-435, ovarian cancer cell line OVCAR-3 and renal cancer cell line A498. Analogues **2m** and **2h** exhibited GI₅₀ values <10nM against leukemia cell lines K-562, SR, non-small lung cancer cell line HOP-92, colon cancer cell lines HCT-116, and HCT-15, melanoma cancer lines M14, and UACC-62, ovarian cancer cell line NCI/ADR-RES and renal cancer cell line A498 Analogue **2e** was evaluated for anti-cancer activity by colony formation assay against 9LSF rat gliosarcoma cells, and afforded an LD₅₀ value of 7.5 nM. A cell cycle redistribution assay with **2e** was also conducted to further understand the mechanism of action of this CA-4 analogue. *In silico* docking studies with compounds **2l**, **2e** and **2h** within the active site of tubulin were carried out in order to rationalize the anticancer properties of these compounds. From these studies, compound **2e** exhibited higher affinity for the colchicine binding site on tubulin compared to **2l** and **2h**. From this study, analogues **2e** and **2l** were considered lead compounds in this new structural class, and worthy of further development as anti-cancer agents.

5.0 Experimental Section

5.1. Chemistry

TLC experiments were carried out on pre-coated silica gel plates (F 254 Merck). ¹H and ¹³C NMR spectra were recorded on a Varian 400 MHz spectrometer equipped with a Linux workstation running on vNMRj software. All spectra were phased, baseline was corrected where necessary, and solvent signals (CDCl₃) were used as reference for both ¹H and ¹³C spectra. HRMS data was obtained on an Agilent 6210 LCTOF instrument operated in multimode.

5.2. General Synthetic procedure for the synthesis of 4,5-disubstituted-2H-1,2,3-triazoles

In the first synthetic step, a series of (Z)-substituted diarylacrylonitrile analogues were synthesized by reacting substituted benzyl carbaldehydes with their corresponding

substituted phenylacetonitriles in 5% NaOMe in methanol. The reaction mixture was stirred at room temperature for 2–3 hours for the reaction to complete and the final product to crash out of the solution. The precipitate is filtered, washed with water and dried to yield the final compounds with yields ranging from 70–95 % (Scheme 1) [16].

In the second synthetic step the 4,5-disubstituted-2*H*-1,2,3-triazoles were synthesized by refluxing a mixture of the (*Z*)-2,3-diarylacrylonitrile (**1a–1s**), NaN₃, and NH₄Cl in a mole ratio of 1:3:3 in 10:1 volumes of DMF/H₂O for 5–12 h. The reaction was monitored by TLC. When the starting material had completely disappeared, cold water was added and the mixture was stirred over 10–15 min, during which time the final product precipitated out and was filtered off. In the absence of a precipitate, the product was extracted into ethyl acetate, the organic extract washed with copious amounts of water, and the resulting organic liquor evaporated to dryness on a rotavaporator. The residue obtained was purified by flash column chromatography to afford the corresponding triazole analogue of CA-4.

In the second synthetic step the 4,5-disubstituted-2*H*-1,2,3-triazoles were synthesized by refluxing a mixture of the (*Z*)-2,3-diarylacrylonitrile (**1a–1s**), NaN₃, and NH₄Cl in a mole ratio of 1:3:3 in 10:1 volumes of DMF/H₂O for 5–12 h. The reaction was monitored by TLC. When the starting material had completely disappeared, cold water was added and the mixture was stirred over 10–15 min, during which time the final product precipitated out and was filtered off. In the absence of a precipitate, the product was extracted into ethyl acetate, the organic extract washed with copious amounts of water, and the resulting organic liquor evaporated to dryness on a rotavaporator. The residue obtained was purified by flash column chromatography to afford the corresponding triazole analogue of CA-4.

5.3. Analytical data of 4,5-disubstituted-2*H*-1,2,3-triazoles

5.3.1. 4-(3,4-dichlorophenyl)-5-(3,4-dimethoxyphenyl)-2*H*-1,2,3-triazole (**2a**)

¹H NMR (400 MHz, CDCl₃): δ 3.82 (s, 3H, -OCH₃), δ 3.93 (s, 3H, -OCH₃), 6.88 (d, *J* = 8 Hz, 1H, ArH), 7.06 (d, *J* = 12 Hz, 2H, ArH), 7.42 (s, 2H, ArH), 7.78 (s, 1H, ArH), 12.49 (bs, 1H, NH) *ppm*. ¹³C NMR (100 MHz, CDCl₃): δ 55.87, 55.96, 111.19, 121.31, 127.31, 129.80, 129.89, 130.54, 132.60, 132.86, 149.15, 149.73 *ppm*. HRMS (ESI): *m/z* calcd for C₁₆H₁₄Cl₂N₃O₂ [M+H]⁺: 350.0463; found 350.0465.

5.3.2. 4,5-bis(3,4,5-trimethoxyphenyl)-2*H*-1,2,3-triazole (**2b**)

¹H NMR (400 MHz, CDCl₃): δ 3.76 (s, 12H, -OCH₃), 3.88 (s, 6H, -OCH₂), 6.84 (s, 4H, ArH), 12.50 (bs, 1H, NH) *ppm*. ¹³C NMR (100 MHz, CDCl₃): δ 56.08, 60.96, 105.57, 125.58, 138.28, 153.27 *ppm*. HRMS (ESI): *m/z* calcd for C₂₀H₂₄N₃O₆ [M+H]⁺: 402.1665; found 402.1668.

5.3.3. 4-(5-(3,4,5-trimethoxyphenyl)-2*H*-1,2,3-triazol-4-yl) quinolone (**2c**)

¹H NMR (400 MHz, CDCl₃): δ 3.47 (s, 6H, -OCH₃), 3.81 (s, 3H, -OCH₃), 6.65 (s, 2H, ArH), 7.50–7.52 (t, *J* = 8 Hz, 1H, ArH), 7.55 (d, *J* = 4.4 Hz, 1H, ArH), 7.77 (t, *J* = 1.6 Hz, 1H, ArH), 7.83 (d, *J* = 8 Hz, 1H, ArH), 8.28 (d, *J* = 8.8 Hz, 1H, ArH), 9.03 (d, *J* = 4.4 Hz, 1H, ArH) *ppm*. ¹³C NMR (100 MHz, CDCl₃): δ 55.70, 60.85, 104.47, 122.68, 122.76, 124.69, 125.95, 126.66, 127.52, 129.42, 130.21, 138.21, 138.45, 148.15, 149.63, 149.69, 153.24 *ppm*. HRMS (ESI): *m/z* calcd for C₂₀H₁₉N₄O₃ [M+H]⁺: 363.1457; found 363.1460.

5.3.4. 2-(5-(3,4,5-trimethoxyphenyl)-2H-1,2,3-triazol-4-yl) quinolone (2d)—¹H NMR (400 MHz, CDCl₃): δ 3.78 (s, 6H, -OCH₃), 3.91 (s, 3H, -OCH₃), 7.08 (s, 2H, ArH), 7.56 (t, *J* = 14.8 Hz, 1H, ArH), 7.72 (t, *J* = 14.8 Hz, 1H, ArH), 7.83 (d, *J* = 6.4 Hz, 2H, ArH), 8.09 (d, *J* = 8.8 Hz, 1H, ArH), 8.17 (d, *J* = 8.4 Hz, 1H, ArH) *ppm*. ¹³C NMR (100 MHz, CDCl₃): δ 56.08, 60.92, 106.21, 120.70, 125.57, 127.12, 127.56, 127.73, 127.68, 129.04, 130.20, 136.83, 138.50, 147.76, 153.19 *ppm*. HRMS (ESI): *m/z* calcd for C₂₀H₁₉N₄O₃ [M+H]⁺: 363.1457; found 363.1456.

5.3.5. 2-methoxy-5-(5-(3,4,5-trimethoxyphenyl)-2H-1,2,3-triazol-4-yl)phenol (2e)—¹H NMR (400 MHz, CDCl₃): δ 3.73 (s, 6H, -OCH₃), 3.88 (s, 6H, -OCH₃), 6.82 (d, *J* = 2 Hz, 3H, ArH), 7.04 (d, *J* = 8.4 Hz, 1H, ArH), 7.20 (s, 1H, ArH) *ppm*. ¹³C NMR (100 MHz, CDCl₃): δ 55.92, 56.98, 56.07, 60.91, 60.98, 105.23, 110.63, 114.72, 120.61, 123.01, 125.74, 138.09, 145.66, 147.10, 153.23 *ppm*. HRMS (ESI): *m/z* calcd for C₁₈H₂₀N₃O₅ [M+H]⁺: 358.1403; found 358.1408.

5.3.6. 4-(4-chloro-3-fluorophenyl)-5-(thiophen-3-yl)-2H-1,2,3-triazole (2f)—¹H NMR (400 MHz, CDCl₃): δ 7.22 (d, *J* = 4.8 Hz, 1H, ArH), 7.32 (d, *J* = 8.4 Hz, 1H, ArH), 7.38–7.41 (m, 3H, ArH), 7.50 (d, *J* = 1.2 Hz, 1H, ArH), 10.5 (bs, 1H, NH) *ppm*. ¹³C NMR (100 MHz, CDCl₃): δ 116.17, 121.32, 124.56, 126.73, 127.01, 129.50, 130.75, 138.32, 141.30, 156.84, 159.31 *ppm*. HRMS (ESI): *m/z* calcd for C₁₂H₈N₃FSCl [M+H]⁺: 280.0111; found 280.0118.

5.3.7. 2-(5-(2,4-dichlorophenyl)-2H-1,2,3-triazol-4-yl)pyridine (2g)—¹H NMR (400 MHz, CDCl₃): δ 7.26 (s, 1H, ArH), 7.39 (d, *J* = 8 Hz, 2H, ArH), 7.49–7.54 (m, 2H, ArH), 7.67 (d, *J* = 6.8 Hz, 1H, ArH), 8.63 (s, 1H, ArH) *ppm*. ¹³C NMR (100 MHz, CDCl₃): δ 121.68, 123.21, 127.27, 129.64, 132.76, 134.74, 135.52, 136.94, 149.45 *ppm*. HRMS (ESI): *m/z* calcd for C₁₃H₉N₄Cl₂ [M+H]⁺: 291.0204; found 291.0201.

5.3.8. 4-(2,3-dihydrobenzo[*b*][1,4]dioxin-6-yl)-5-(3,4,5-trimethoxyphenyl)-2H-1,2,3-triazole (2h)—¹H NMR (400 MHz, CDCl₃): δ 3.77 (s, 6H, 2xOCH₃), 3.89 (s, 3H, OCH₃), 4.26–4.29 (m, 2xCH₂), 6.84 (s, 2H, ArH), 6.88 (d, 1H, *J* = 8 Hz, Ar-H), 7.04–7.07 (dd, 1H, *J* = 2 and 8 Hz, 1H, Ar-H), 7.15 (d, 1H, Ar-H), 12.2 (bs, 1H, NH) *ppm*. ¹³C NMR (100 MHz, CDCl₃): δ 55.99, 60.99, 64.27, 105.24, 105.28, 117.42, 121.80, 138.18, 143.59, 144.09, 153.26 *ppm*. HRMS (ESI): *m/z* calcd for C₁₉H₂₀N₃O₅ [M+H]⁺: 370.1403; found 370.1398.

5.3.9. 4-(4-nitrophenyl)-5-(3,4,5-trimethoxyphenyl)-2H-1,2,3-triazole (2i)—¹H NMR (400 MHz, DMSO-*d*₆): δ 3.70–3.72 (d, 9H, -OCH₃), 6.80 (s, 2H, ArH), 7.86 (s, 2H, ArH), 8.30 (d, *J* = 8.4 Hz, 2H, ArH) *ppm*. ¹³C NMR (100 MHz, DMSO-*d*₆): 56.23, 61.06, 105.75, 123.91, 128.76, 137.57, 138.73, 147.50, 153.62 *ppm*. HRMS (ESI): *m/z* calcd for C₁₇H₁₇N₄O₅ [M+H]⁺: 357.1199; found 357.1199.

5.3.10. 4-(benzo[*d*][1,3]dioxol-5-yl)-5-phenyl-2H-1,2,3-triazole (2j)—¹H NMR (400 MHz, CDCl₃): δ 6.00 (s, 2H, -CH₂), 6.81 (d, *J* = 8.8 Hz, 1H, ArH), 7.04 (d, *J* = 6.8 Hz, 2H, ArH), 7.39 (t, *J* = 5.2 Hz, 3H, ArH), 7.57 (m, *J* = 9.6 Hz, 1H, ArH) *ppm*. ¹³C NMR (100 MHz, CDCl₃): δ 101.43, 108.77, 108.91, 122.46, 123.96, 128.41, 128.73, 128.88, 130.25,

142.29, 148.01, 148.11 ppm. HRMS (ESI): m/z calcd for $C_{15}H_{12}N_3O_2$ $[M+H]^+$: 266.0930; found 266.0928.

5.3.11. 4-(3,5-dibromophenyl)-5-(2-methoxyphenyl)-2H-1,2,3-triazole (2k)— 1H NMR (400 MHz, $CDCl_3$): δ 3.76 (s, 3H, $-OCH_3$), 7.04 (d, $J = 4.8$ Hz, 2H, ArH), 7.39–7.47 (m, 2H, ArH), 7.63 (d, $J = 1.6$ Hz, 1H, ArH), 7.71 (s, 2H, ArH), 12.2 (bs, 1H, NH) ppm. ^{13}C NMR (100 MHz, $CDCl_3$): δ 55.51, 111.54, 121.21, 122.83, 129.17, 130.48, 131.29, 133.34, 133.42, 134.96, 156.51 ppm. HRMS (ESI): m/z calcd for $C_{15}H_{12}N_3O$ Br_2 $[M+H]^+$: 407.9347; found 407.9342.

5.3.12. 4-(4-methoxyphenyl)-5-(3,4,5-trimethoxyphenyl)-2H-1,2,3-triazole (2l)— 1H NMR (400 MHz, $CDCl_3$): δ 3.74 (s, 6H, $-OCH_3$), 3.84 (s, 3H, $-OCH_3$), 3.89 (s, 3H, $-OCH_3$), 6.83 (s, 2H, ArH), 6.92 (d, $J = 8.4$ Hz, 2H, ArH), 7.52 (d, $J = 8.0$ Hz, 2H, ArH), 12.2 (bs, 1H, NH) ppm. ^{13}C NMR (100 MHz, $CDCl_3$): δ 55.27, 55.96, 60.90, 105.14, 105.18, 114.03, 125.86, 129.79, 138.07, 153.27, 159.97 ppm. HRMS (ESI): m/z calcd for $C_{18}H_{20}N_3O_4$ $[M+H]^+$: 342.1454; found 342.1448.

5.3.13. 4-(3,5-dimethoxyphenyl)-5-(4-methoxyphenyl)-2H-1,2,3-triazole (2m)— 1H NMR (400 MHz, $DMSO-d_6$): δ 3.68 (s, 6H, $-OCH_3$), 3.78 (s, 3H, $-OCH_3$), 6.5 (s, 1H, Ar-H), 6.64 (2H, Ar-H), 7.01 (d, 2H, $J = 8$ Hz, ArH), 7.43 (d, 2H, $J = 8.8$ Hz, Ar-H), HRMS (ESI): m/z calcd for $C_{17}H_{18}N_3O_3$ $[M+H]^+$: 312.1348; found 312.1344.

5.3.14. 4-(benzo[d][1,3]dioxol-5-yl)-5-(3,4,5-trimethoxy phenyl)-2H-1,2,3-triazole (2n)— 1H NMR (400 MHz, $CDCl_3$): δ 3.77 (s, 6H, $-OCH_3$), 3.89 (s, 3H, $-OCH_3$), 4.26–4.29 (q, $J = 12.4$ Hz, 4H, ArH), 6.84 (s, 2H, ArH), 6.88 (d, $J = 8$ Hz, 1H, ArH), 7.04–7.07 (dd, $J = 2$ Hz, 8 Hz, 1H, ArH), 7.16 (d, $J = 1.6$ Hz, 1H, ArH), 7.26 (s, 1H, ArH) ppm. ^{13}C NMR (100 MHz, $CDCl_3$): δ 55.99, 56.08, 60.90, 60.99, 64.27, 64.47, 105.24, 105.28, 117.42, 121.80, 138.18, 143.59, 144.09, 153.26 ppm. HRMS (ESI): m/z calcd for $C_{18}H_{18}N_3O_5$ $[M+H]^+$: 356.1246; found 356.1248.

5.3.15. 4-(3,4-dichlorophenyl)-5-(3,4,5-trimethoxyphenyl)-2H-1,2,3-triazole (2o)— 1H NMR (400 MHz, $CDCl_3$): δ 3.79 (s, 6H, $-OCH_3$), 3.91 (s, 3H, $-OCH_3$), 6.77 (s, 2H, ArH), 7.46 (s, 2H, ArH), 7.82 (s, 1H, ArH) ppm. ^{13}C NMR (100 MHz, $CDCl_3$): δ 56.14, 60.98, 105.49, 127.51, 129.92, 130.57, 132.51, 132.77, 138.46, 153.47 ppm. HRMS (ESI): m/z calcd for $C_{17}H_{16}Cl_2N_3O_3$ $[M+H]^+$: 380.0569; found 380.0564.

5.3.16. 2-(5-(3,4,5-trimethoxyphenyl)-2H-1,2,3-triazol-4-yl)pyridine (2p)— 1H NMR (400 MHz, $CDCl_3$): δ 3.81 (s, 6H, $-OCH_3$), 3.90 (s, 3H, $-OCH_3$), 6.9 (s, 2H, ArH), 7.28 (d, $J = 12.8$ Hz, 2H, ArH), 7.70 (s, 2H, ArH), 8.67 (s, 1H, ArH) ppm. ^{13}C NMR (100 MHz, $CDCl_3$): δ 56.10, 60.94, 106.04, 123.22, 123.46, 125.66, 137.06, 138.37, 149.36, 153.26 ppm. HRMS (ESI): m/z calcd for $C_{16}H_{17}N_4O_3$ $[M+H]^+$: 313.1301; found 313.1298.

5.3.17. 4-(3,5-dimethoxyphenyl)-5-(4-nitrophenyl)-2H-1,2,3-triazole (2q)— 1H NMR (400 MHz, $CDCl_3$): δ 3.74 (s, 6H, $-OCH_3$), 6.51 (d, $J = 1.2$ Hz, 1H, ArH), 6.62 (s, 2H, ArH), 7.8 (d, $J = 8.4$ Hz, 2H, ArH), 8.19 (d, $J = 8.4$ Hz, 2H, Ar-H) ppm. ^{13}C NMR (100

MHz, CDCl₃): δ 55.43, 101.28, 106.53, 123.85, 128.67, 137.08, 147.49, 161.13 ppm. HRMS (ESI): *m/z* calcd for C₁₆H₁₅N₄O₄ [M+H]⁺: 327.1093; found 327.1084.

5.3.18. 4-(benzo[d][1,3]dioxol-5-yl)-5-(3,5-dimethoxyphenyl)-2H-1,2,3-triazole (2r)—¹H NMR (400 MHz, CDCl₃): δ 3.75 (s, 6H, -OCH₃), 5.99 (s, 2H, ArH), 6.48 (s, 1H, ArH), 6.73(d, *J* = 2.4 Hz, 2H, ArH), 6.82 (d, *J* = 8.8 Hz, 1H, ArH), 7.06 (d, *J* = 6.4 Hz, 2H, ArH), 12.1 (bs, 1H, NH) ppm. ¹³C NMR (100 MHz, CDCl₃): δ 55.34, 55.51, 101.05, 101.25, 106.12, 108.51, 108.80, 122.38, 131.91, 147.81, 147.98, 160.87 ppm. HRMS (ESI): *m/z* calcd for C₁₇H₁₆N₃O₄ [M+H]⁺: 326.1141; found 326.1133.

5.3.19. 2-(5-(benzo[d][1,3]dioxol-5-yl)-2H-1,2,3-triazol-4-yl)pyridine (2s)—¹H NMR (400 MHz, CDCl₃): δ 5.99 (s, 2H, -CH₂), 6.83 (d, *J* = 8.4 Hz, 1H, ArH), 7.14 (d, *J* = 6 Hz, 2H, ArH), 7.27 (d, *J* = 8.4 Hz, 1H, ArH), 7.70 (d, *J* = 7.2 Hz, 2H, ArH), 8.69 (s, 1H, ArH) ppm. ¹³C NMR (100 MHz, CDCl₃): δ 101.15, 101.25, 101.35, 108.52, 109.31, 109.34, 122.78, 123.30, 124.04, 137.02, 147.77, 148.06, 149.56 ppm. HRMS (ESI): *m/z* calcd for C₁₄H₁₁N₄O₂ [M+H]⁺: 267.0882; found 267.0879.

Supplementary Material

Refer to Web version on PubMed Central for supplementary material.

Acknowledgements

We are grateful for support from NCI/NIH Grants CA 140409 (to P.A.C.) and CA 183895 (to R.L.E.), the UAMS Translational Research Institute (TRI), grant UL1TR000039 through the NIH National Center for Research Resources and National Center for Advancing Translational Sciences, the UAMS Department of Radiology the Arkansas Research Alliance (ARA), and to the NCI Developmental Therapeutic Program (DTP) for screening data.

Notes and references

1. Gordaliza M. Natural products as leads to anticancer drugs. *Clin. Transl. Oncol.* 2007; 9:767–776. [PubMed: 18158980]
2. Jordan MA. Mechanism of action of antitumor drugs that interact with microtubules and tubulin. *Curr. Med. Chem.: Anti-Cancer Agents.* 2002; 2:1–17. [PubMed: 12678749]
3. Hadfield JA, Ducki S, Hirst N, McGown AT. Tubulin and microtubules as targets for anticancer drugs. *Prog. Cell. Cycle. Res.* 2003; 5:309–325. [PubMed: 14593726]
4. Jordan MA, Wilson L. Microtubules as a target for anticancer drugs. *Nat. Rev. Cancer.* 2004; 4:253–265. [PubMed: 15057285]
5. Young SL, Chaplin DJ. Combretastatin-A4 phosphate: background and current clinical status. *Expert. Opin. Investig. Drugs.* 2004; 13:1171–1182.
6. Cooney MM, Ortiz J, Bukowski RM, Remick SC. Novel vascular targeting/disrupting agents: combretastatin-A4 phosphate and related compounds. *Curr. Oncol. Rep.* 2005; 7:90–95. [PubMed: 15717941]
7. Tron GC, Pirali T, Sorba G, Pagliai F, Busacca S, Genazzani AA. Medicinal chemistry of combretastatin-A4: present and future directions. *J. Med. Chem.* 2006; 49:3033–3044. [PubMed: 16722619]
8. Tozer GM, Kanthou C, Parkins CS, Hill SA. The biology of the combretastatins as tumour vascular targeting agents. *Int. J. Exp. Pathol.* 2002; 83:21–38. [PubMed: 12059907]
9. Hsieh HP, Liou JP, Mahindroo N. Pharmaceutical design of anti-mitotic agents based on combretastatins. *Curr. Pharm. Des.* 2005; 11:1655–1677. [PubMed: 15892667]

10. Carr M, Greene LM, Knox AJS, Lloyd DG, Zisterer DM, Meegan MJ. Lead identification of conformationally restricted β -lactam type combretastatin analogues: Synthesis, antiproliferative activity and tubulin targeting effects. *Eur. J. Med. Chem.* 2010; 45:5752–5766. [PubMed: 20933304]
11. Banimustafa M, Kheirollahi A, Safavi M, Kabudanian Ardestani S, Aryapour H, Foroumadi A, Emami S. Synthesis and biological evaluation of 3-(trimethoxyphenyl)-2(3*H*)-thiazole thiones as combretastatin analogs. *Eur. J. Med. Chem.* 2013; 70:692–702. [PubMed: 24219991]
12. Beale TM, Bond PJ, Brenton JD, Charnock-Jones DS, Ley SV, Myers RM. Increased endothelial cell selectivity of triazole-bridged dihalogenated A-ring analogues of combretastatin A-1. *Bioorg. Med. Chem.* 2012; 20:1749–1759. [PubMed: 22304851]
13. Demchuk DV, Samet AV, Chernysheva NB, Ushkarov VI, Stashina GA, Konyushkin LD, Raihstat MM, Firgang SI, Philchenkov AA, Zavelevich MP, Kuiava LM, Chekhun VF, Blokhin DY, Kiselyov AS, Semenova MN, Semenov VV. Synthesis and antiproliferative activity of conformationally restricted 1,2,3-triazole analogues of combretastatins in the sea urchin embryo model and against human cancer cell lines. *Bioorg. Med. Chem.* 2014; 22:738–755. [PubMed: 24387982]
14. Shirai R, Takayama H, Nishikawa A, Koiso Y, Hashimoto Y. Asymmetric synthesis of antimetabolic combretadioxolane with potent antitumor activity against multidrug resistant cells. *Bioorg. Med. Chem. Lett.* 1998; 8:1997–2000. [PubMed: 9873473]
15. Tron GC, Pagliai F, Del Grosso E, Genazzani AA, Sorba G. Synthesis and cytotoxic evaluation of combretafurazans. *J. Med. Chem.* 2005; 48:3260–3268. [PubMed: 15857132]
16. Penthala NR, Zong H, Ketkar A, Madadi NR, Janganati V, Eoff RL, Guzman ML, Crooks PA. Synthesis, anticancer activity and molecular docking studies on a series of heterocyclic *trans*-cyanocombretastatin analogues as antitubulin agents. *Eur. J. Med. Chem.* 2015; 92:212–220. [PubMed: 25557492]
17. Madadi NR, Penthala NR, Song L, Hendrickson HP, Crooks PA. Preparation of 4,5-disubstituted-2*H*-1,2,3-triazoles from (*Z*)-2,3-diaryl substituted acrylonitriles. *Tetrahedron Lett.* 2014; 55:4207–4211.
18. Madadi NR, Penthala NR, Bommagani S, Parkin S, Crooks PA. Crystal structure of 4,5-bis-(3,4,5-trimethoxyphenyl)-2*H*-1,2,3-triazole methanol monosolvate. *Acta. Crystallogr. Sect. E: Struct. Rep. Online.* 2014; 70:o1128–o1129.
19. Penthala NR, Madadi NR, Bommagani S, Parkin S, Crooks PA. Comparison of crystal structures of 4-(benzo[*b*]thio-phen-2-yl)-5-(3,4,5-trimethoxyphenyl)-2*H*-1,2,3-triazole and 4-(benzo[*b*]thiophen-2-yl)-2-methyl-5-(3,4,5-trimethoxyphenyl)-2*H*-1,2,3-triazole. *Acta. Crystallogr. Sect. E: Struct. Rep. Online.* 2014; 70:392–395.
20. Penthala NR, Madadi NR, Janganati V, Crooks PA. L-Proline catalyzed one-step synthesis of 4,5-diaryl-2-1,2,3-triazoles from heteroaryl cyanostilbenes via [3+2] cycloaddition of azide. *Tetrahedron Lett.* 2014; 55:5562–5565. [PubMed: 25267862]
21. Nam NH. Combretastatin-A4 analogues as anti-mitotic antitumor agents. *Curr. Med. Chem.* 2003; 10:1697–1722. [PubMed: 12871118]
22. Rubinstein LV, Shoemaker RH, Paull KD, Simon RM, Tosini S, Skehan P, Scudiero DA, Monks A, Boyd MR. Comparison of in vitro anticancer-drug-screening data generated with a tetrazolium assay versus a protein assay against a diverse panel of human tumor cell lines. *J. Natl. Cancer. Inst.* 1990; 82:1113–1118. [PubMed: 2359137]
23. Madadi NR, Penthala NR, Janganati V, Crooks PA. Synthesis and anti-proliferative activity of aromatic substituted 5-((1-benzyl-1*H*-indol-3-yl) methylene)-1,3-dimethylpyridine-2, 4, 6 (1*H*, 3*H*, 5*H*)-trione analogs against human tumor cell lines. *Bioorg. Med. Chem. Lett.* 2014; 24:601–603. [PubMed: 24361000]
24. Madadi NR, Zong H, Ketkar A, Zheng C, Penthala NR, Janganati V, Bommagani S, Eoff RL, Guzman ML, Crooks PA. Synthesis and evaluation of a series of resveratrol analogues as potent anti-cancer agents that target tubulin. *Med. Chem. Comm.* 2015; 6:788–794.
25. Borrelli MJ, Stafford DM, Rausch CM, Bernock LJ, Freeman ML, Lepock JR, Corry PM. Diamide-induced cytotoxicity and thermotolerance in CHO cells. *J. Cell. Physiol.* 1998; 177:483–492. [PubMed: 9808156]

26. Borrelli MJ, Thompson LL, Dewey WC. Evidence that the feeder effect in mammalian cells is mediated by a diffusible substance. *Int. J. Hyperthermia*. 1989; 5:99–103. [PubMed: 2646382]
27. Grosdidier A, Zoete V, Michielin O. SwissDock, a protein-small molecule docking web service based on EADock DSS. *Nucleic Acids Res*. 2011; 39:W270–W277. [PubMed: 21624888]

Highlights

- A variety of novel 4,5-disubstituted 2H-1,2,3-triazoles were synthesized from their corresponding (Z)-substituted diarylacrylonitriles.
- The synthesized analogs were evaluated for their anti-cancer activity against NCI 60 human cancer cell lines.
- Conducted *in silico* docking studies to rationalize the anti-cancer properties of the synthesized compounds.
- Cell cycle redistribution assay was conducted to further understand the mechanism of action of the synthesized CA-4 analogues.
- One of the analogues **2e** showed promising anticancer activity with an LD₅₀ value of 7.5 nM against 9LSF rat gliosarcoma cells.

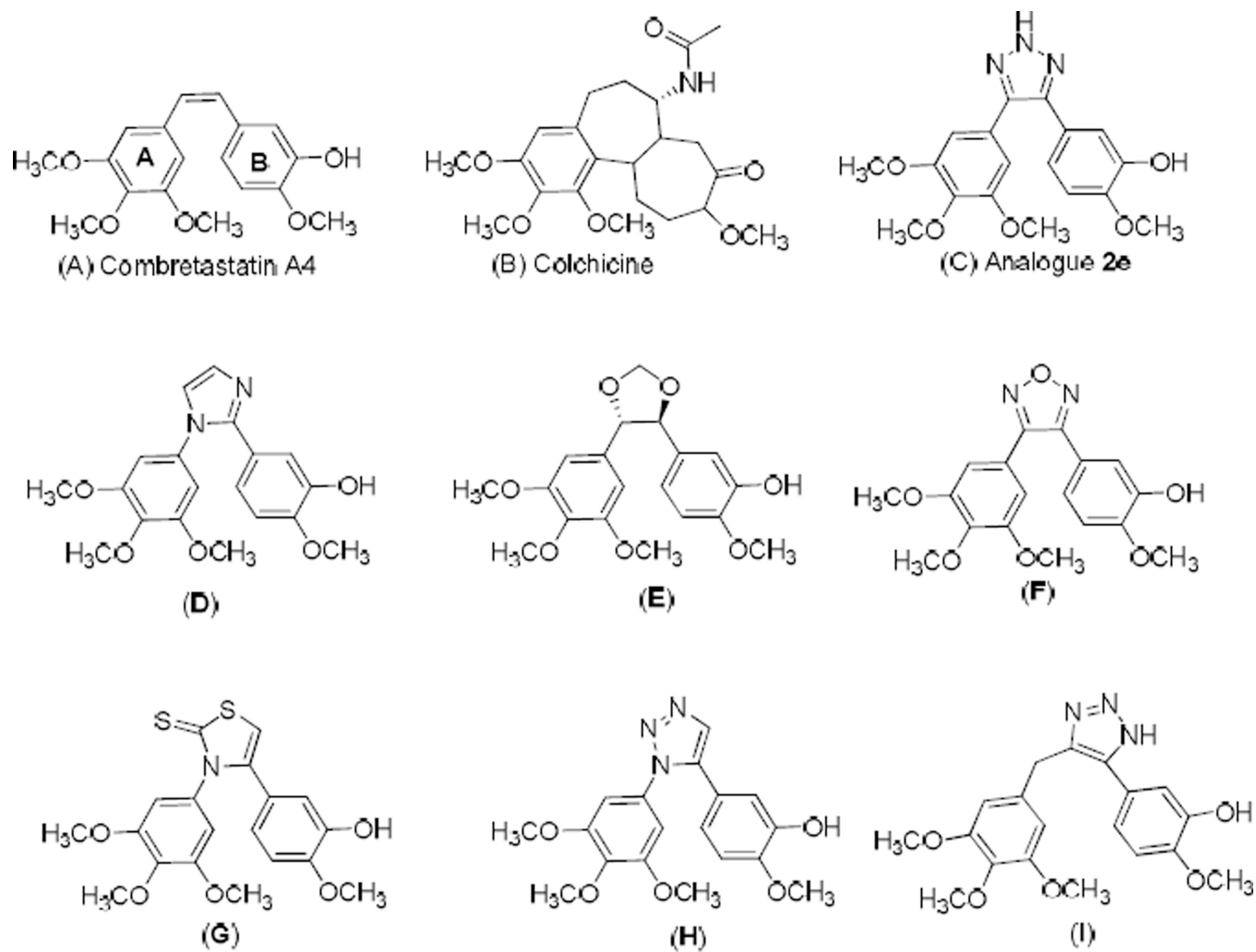


Fig. 1. Structures of combretastatin A-4 (CA-4, **A**), colchicine (**B**), triazole analogue (**2e**, **C**) and reported anti-tubulin compounds (**D–I**).

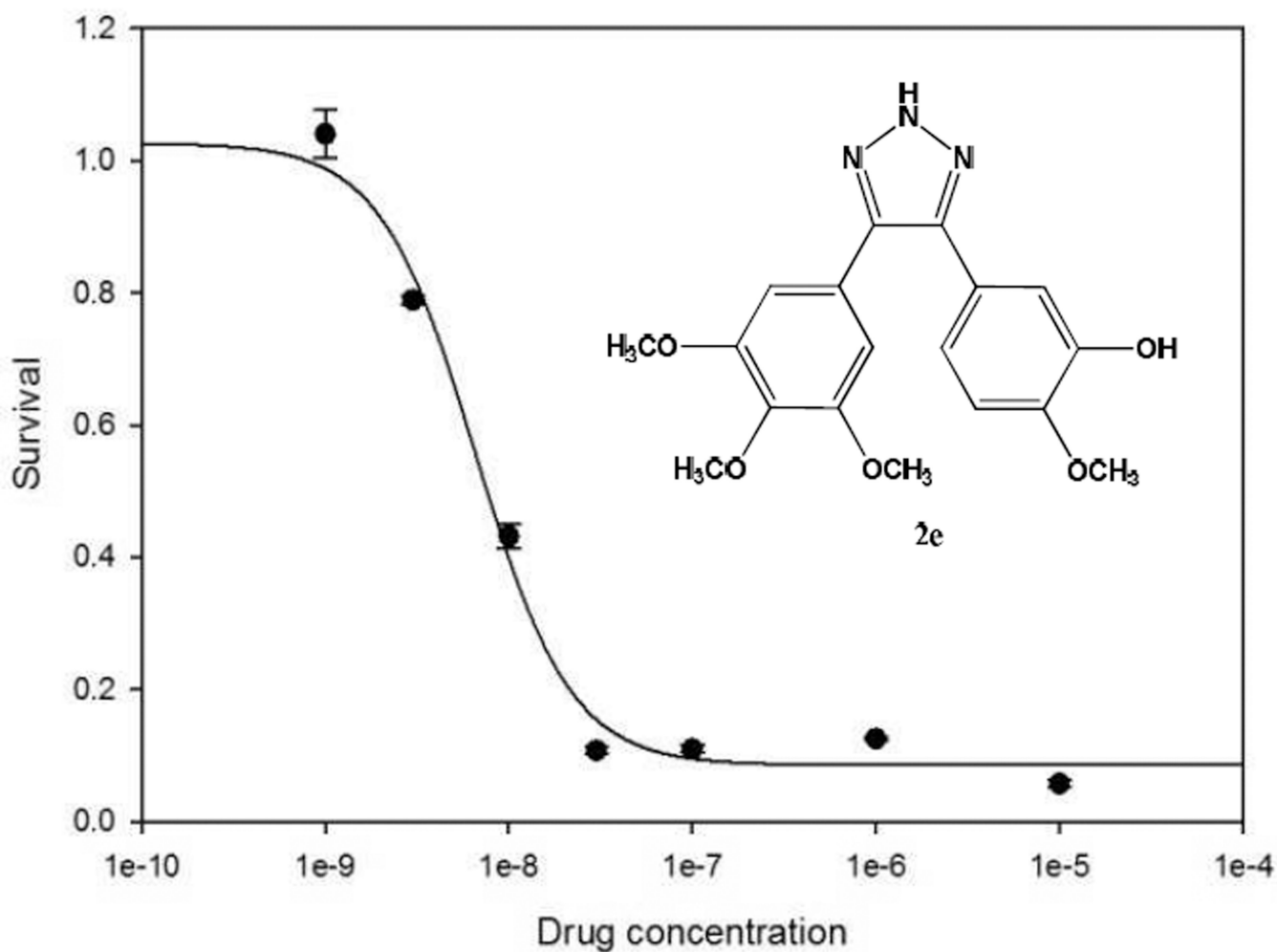


Fig. 2. Colony formation assay, **2e**-treated 9LSF cells. Cells were exposed to **2e** for 24 hours. Curve was fitted as four-parameter logistic curve ($f1 = \min + (\max - \min) / (1 + (x / EC50)^{-Hillslope})$). Values represent mean \pm SEM of 3 independent colony formation experiments.

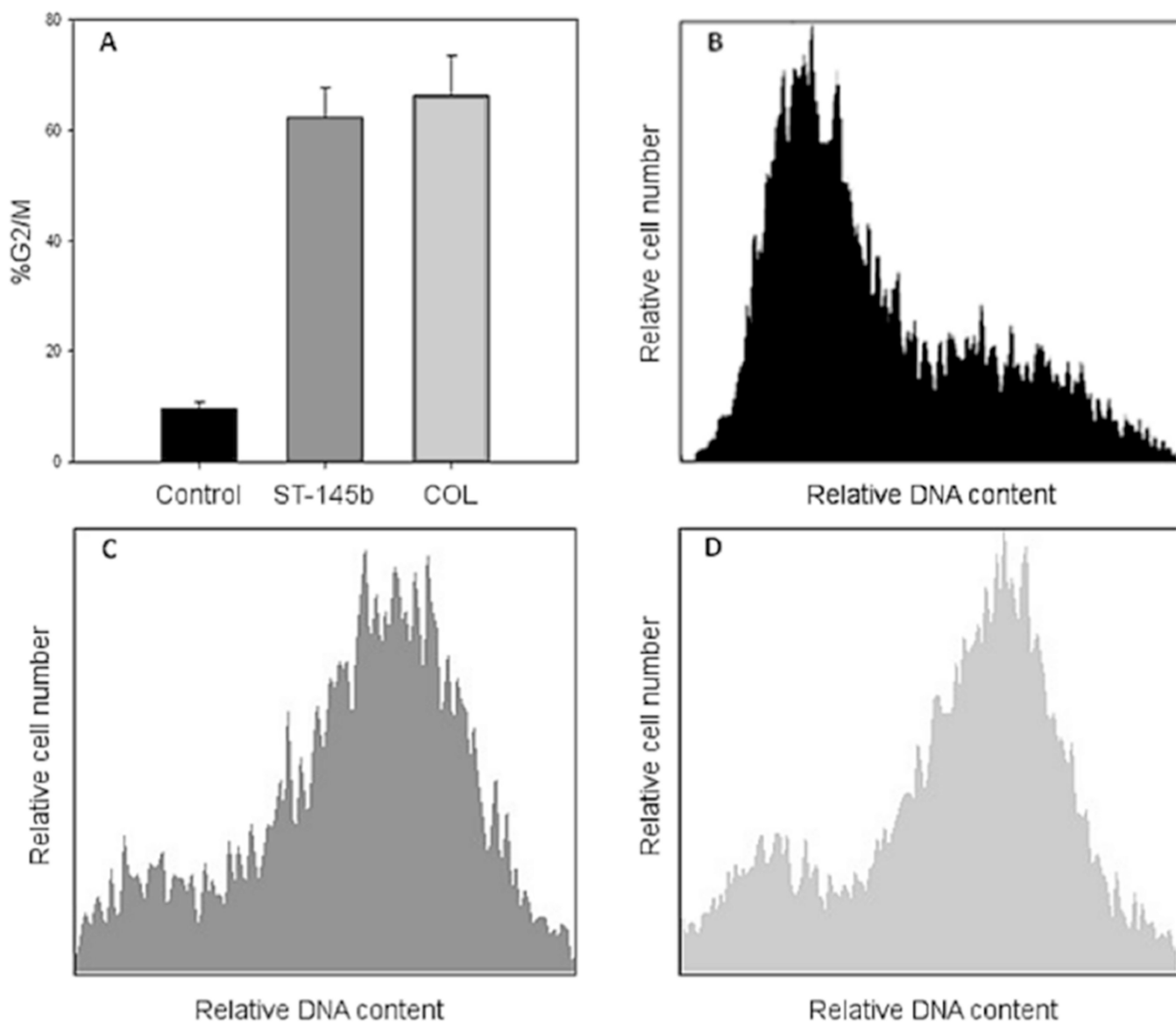


Fig 3. Cell cycle redistribution effects of **2e** on 9L cells. (A) Percentage of cell population in G2/M phase in control cells versus those exposed to 50 μ M **2e** or 50 μ M COL for 24 hrs. (B) Representative distribution of control cells. (C) Representative distribution of **2e**-treated cells. (D) Representative distribution of COL-treated cells.

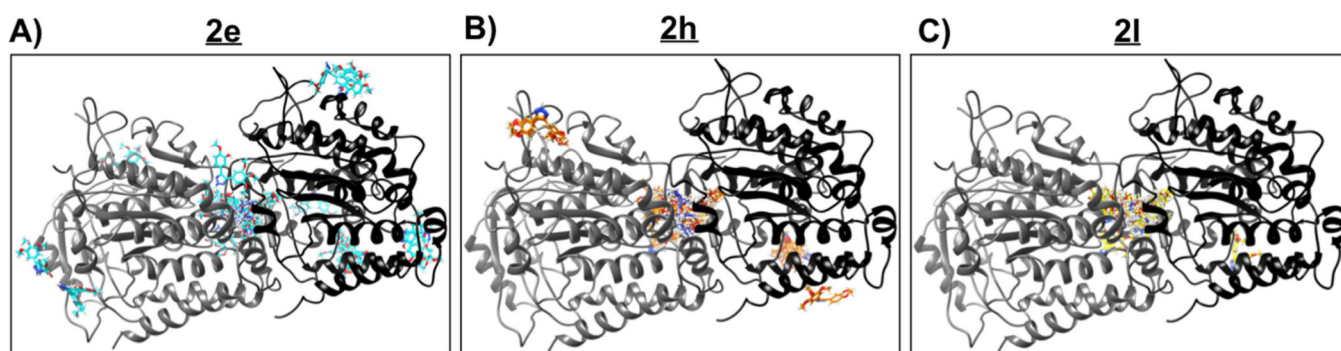


Fig. 4. Docking poses of molecules **2e**, **2h** and **2l** bound to tubulin. Subunits α and β of the tubulin heterodimer are shown as *gray* and *black* cartoons respectively. All the docking poses generated by Swissdock for molecules **2e**, **2h** and **2l** are shown in panels **A**), **B**) and **C**) respectively. As seen clearly, majority of the poses bind to the ‘colchicine-binding’ pocket located at the interface of the two tubulin subunits for all three molecules. **2e** shows the most, while **2l** shows the least number of ‘outlier’ poses.

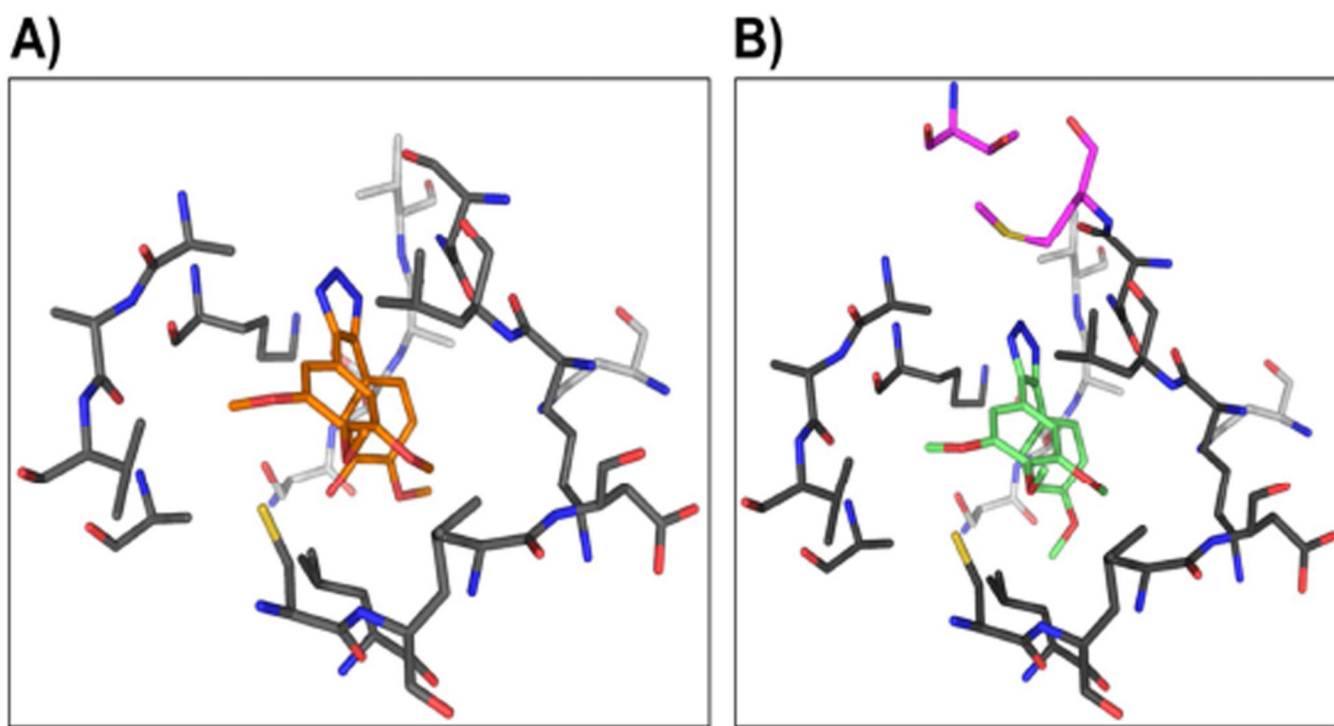
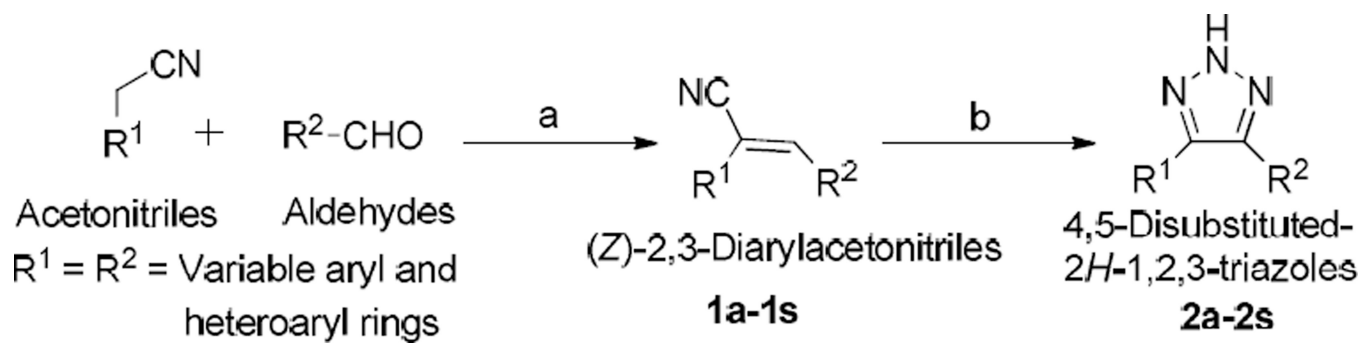


Fig. 5. Atomic contacts between tubulin and molecules **2e** and **2l**. A) **2e** is shown as *orange* sticks, while residues of the α and β subunit of tubulin are in *light* and *dark gray*, respectively. B) **2l** (*green* sticks) is shown bound at the colchicine-binding pocket of tubulin. The color scheme is the same as in A, while the residues of β -tubulin unique to **2l** pocket are shown in *magenta*.

**Scheme 1.**

Synthesis of 4,5-disubstituted 2H-1,2,3-triazoles; reagents and conditions: (a) 5% NaOMe, MeOH, reflux. (b) NaN_3 , NH_4Cl , DMF/ H_2O .

Table 1

Synthesized (Z)-2,3-diarylacrylonitriles and 4,5-disubstituted-2H-1,2,3-triazoles from their corresponding acetonitrile and aldehyde precursors.

| Acetonitrile | Aldehyde | (Z)-2,3-Diarylacetonitriles (1a-1s) | 4,5-Disubstituted 2H-1,2,3-triazoles (2a-2s) |
|--------------|----------|-------------------------------------|--|
| | | | |
| | | | |
| | | | |
| | | | |
| | | | |
| | | | |
| | | | |
| | | | |
| | | | |

Author Manuscript

Author Manuscript

Author Manuscript

Author Manuscript

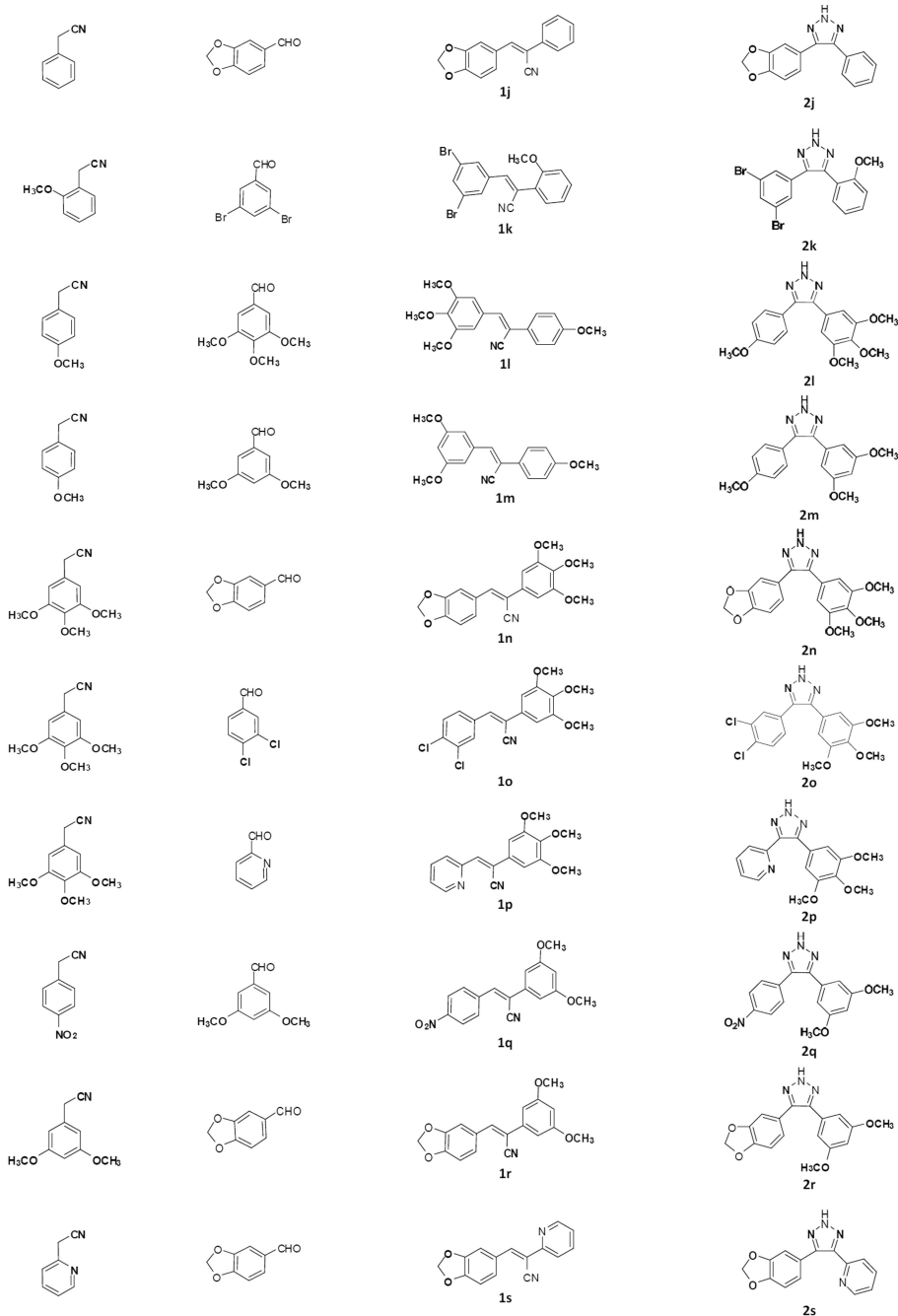


Table 2

Growth inhibition ($GI_{50}/\mu M$)^a data of **2d**, **2m**, **2l**, **2n** and **2g** against a panel of 60 human cancer cells.

| Panel/cell line | 2d (μM) | 2m (μM) | 2l (μM) | 2h (μM) | 2n (μM) | 2g (μM) |
|---------------------|-------------------|-------------------|-------------------|-------------------|-------------------|-------------------|
| <i>Leukemia</i> | | | | | | |
| CCRF-CEM | 0.037 | 0.032 | <0.01 | 0.034 | 0.28 | 3.38 |
| HL-60(TB) | 0.030 | 0.023 | <0.01 | 0.019 | 0.20 | 5.75 |
| K-562 | 0.026 | <0.01 | <0.01 | <0.01 | 0.05 | 5.50 |
| MOLT-4 | 0.068 | 0.048 | 0.012 | 0.040 | 0.57 | 4.23 |
| RPMI-8226 | 0.037 | 0.037 | <0.01 | 0.033 | 0.33 | 10.7 |
| SR | 0.021 | <0.01 | <0.01 | <0.01 | 0.04 | 5.43 |
| <i>Lung Cancer</i> | | | | | | |
| A549/ATCC | 0.054 | 0.037 | <0.01 | 0.023 | 0.29 | 4.85 |
| HOP-62 | 0.047 | 0.025 | <0.01 | 0.018 | 0.34 | 5.32 |
| HOP-92 | 0.099 | <0.01 | <0.01 | <0.01 | 0.12 | 3.28 |
| NCI-H23 | 0.065 | 0.038 | <0.01 | 0.048 | 0.77 | 9.13 |
| NCI-H460 | 0.038 | 0.034 | <0.01 | 0.025 | 0.34 | 3.67 |
| <i>Colon Cancer</i> | | | | | | |
| COLO 205 | 0.228 | 0.149 | 0.029 | 0.027 | 0.31 | 2.89 |
| HCC-2998 | 0.230 | 0.046 | 0.024 | 0.039 | >100 | 9.16 |
| HCT-116 | 0.040 | <0.01 | <0.01 | <0.01 | 0.18 | 2.89 |
| HCT-15 | 0.037 | <0.01 | <0.01 | <0.01 | 0.13 | 2.93 |
| HT29 | 0.214 | 0.048 | <0.01 | 0.025 | 0.39 | 4.56 |
| KM12 | 0.035 | 0.030 | <0.01 | <0.01 | 0.07 | 6.87 |
| SW-620 | 0.041 | 0.030 | <0.01 | <0.01 | 0.11 | 4.40 |
| <i>CNS Cancer</i> | | | | | | |
| SF-268 | 0.503 | 0.177 | <0.01 | 0.069 | >100 | 7.36 |
| SF-295 | 0.014 | 0.011 | <0.01 | <0.01 | 0.10 | 3.01 |
| SF-539 | 0.020 | 0.014 | <0.01 | <0.01 | 0.18 | na |
| SNB-75 | 0.016 | 0.014 | <0.01 | <0.01 | 0.08 | 1.58 |
| U251 | 0.037 | 0.038 | <0.01 | 0.020 | 0.30 | 5.35 |
| <i>Melanoma</i> | | | | | | |

| Panel/cell line | 2d (μ M) | 2m (μ M) | 2l (μ M) | 2h (μ M) | 2n (μ M) | 2g (μ M) |
|------------------------|------------------|------------------|------------------|------------------|------------------|------------------|
| LOX IMVI | 0.065 | 0.076 | <0.01 | 0.018 | 0.55 | 4.83 |
| M14 | 0.022 | <0.01 | <0.01 | <0.01 | na | 14.3 |
| MDA-MB-435 | <0.01 | <0.01 | <0.01 | <0.01 | 0.09 | 2.20 |
| SK-MEL-2 | 0.027 | 0.056 | <0.01 | <0.01 | 0.02 | 6.52 |
| SK-MEL-28 | >100 | na | na | >100 | 0.24 | 5.39 |
| SK-MEL-5 | 0.013 | 0.027 | <0.01 | <0.01 | >100 | 7.89 |
| UACC-62 | 0.157 | <0.01 | nd | >100 | >100 | 3.35 |
| <i>Ovarian Cancer</i> | | | | | | |
| IGROV1 | 0.065 | 0.051 | <0.01 | 0.033 | >100 | 5.94 |
| OVCAR-3 | 0.011 | 0.024 | <0.01 | <0.01 | 0.43 | 3.38 |
| OVCAR-4 | 0.077 | na | <0.01 | 0.034 | 0.08 | 3.04 |
| NCI/ADR-RES | 0.023 | <0.01 | <0.01 | <0.01 | 0.08 | 3.92 |
| SK-OV-3 | 0.075 | 0.046 | <0.01 | <0.01 | 0.49 | 2.72 |
| <i>Renal Cancer</i> | | | | | | |
| 786-0 | 0.043 | 0.015 | <0.01 | <0.01 | 0.62 | 2.75 |
| A498 | 0.033 | <0.01 | <0.01 | 0.010 | 0.34 | 3.18 |
| ACHN | 0.081 | 0.145 | <0.01 | <0.01 | 0.71 | 1.75 |
| CAKI-1 | 0.043 | 0.050 | <0.01 | <0.01 | 0.32 | 8.42 |
| UO-31 | 0.092 | 0.020 | <0.01 | <0.01 | 0.66 | 6.84 |
| <i>Prostate Cancer</i> | | | | | | |
| PC-3 | 0.046 | 0.042 | <0.01 | 0.018 | 0.26 | 4.50 |
| DU-145 | 0.027 | 0.045 | <0.01 | 0.025 | 0.35 | 1.41 |
| <i>Breast Cancer</i> | | | | | | |
| MCF7 | 0.027 | 0.025 | <0.01 | <0.01 | 0.08 | 2.58 |
| MDA-MB-231/ATCC | 0.094 | 0.046 | <0.01 | 0.044 | 0.53 | 5.89 |
| HS 578T | na | 0.041 | <0.01 | 0.668 | 0.44 | 11.6 |
| MDA-MB-468 | 0.035 | 0.023 | <0.01 | 0.015 | 0.23 | 3.20 |

na: Not analyzed, nd; not determined.

^aGI50: 50% growth inhibition, concentration of drug resulting in a 50% reduction in net cell growth as compared to cell numbers on day 0.

Table 3

SwissDock statistics for the docking runs with compounds **2e**, **2h** and **2l** (scores shown are averages from 3 docking runs).

| Comp | FF score (kcal/mol) | G (kcal/mol) |
|-----------|---------------------|--------------|
| 2l | -4224.7 | -8.4 |
| 2h | -4216.5 | -8.2 |
| 2e | -4211.4 | -7.9 |

Author Manuscript

Author Manuscript

Author Manuscript

Author Manuscript